Energy Sources, Part A: Recovery, Utilisation and Environmental Effects
Available online 11 January 2021
DOI:10.1080/15567036.2020.1871449

Influence of coalification on methane diffusion dynamics in middle-high rank coals

Jingyu Jiang[a,b,c*], Ke Zhao[a,b], Phil Longhurst[c**], Yuanping Cheng[a,b], Deyang Wang[a,b]

[a] *Key Laboratory of Gas and Fire Control for Coal Mines (China University of Mining and Technology), Ministry of Education, Xuzhou, 221116, China*

[b] *School of Safety Engineering, China University of Mining and Technology, Xuzhou, Jiangsu 221116, China*

[C] *School of Water, Energy and Environment, Cranfield University, Bedford, MK43 0AL, UK*

* Corresponding author. School of Safety Engineering, China University of Mining and Technology, Xuzhou, Jiangsu 221116, China.

** Corresponding author. School of Water, Energy and Environment, Cranfield University, Bedford, MK43 0AL, UK.

E-mail addresses: jiangjingyu@cumt.edu.cn(J. Jiang), p.j.longhurst@cranfield.ac.uk (P. Longhurst).

Abstract: Understanding the influence of coalification on the diffusion of methane in middle-high rank coals (MHRC) is fundamental for optimizing the coalbed methane (CBM) drainage strategies. Safe coal mining relies critically on this approach. Hence, CH_4 adsorption/desorption experiments and a new methane diffusion model were used to study methane diffusion behavior in five different metamorphic degree coals from China. The results show that, as the vitrinite reflectance (R_o) increase, the Langmuir volume (V_L) tends to decrease at first, and then increase. Coalification especially for the third coalification jump (R_o = 1.26%) shows a turning effect on diffusion dynamics of MHRC. The desorption volume and initial diffusion coefficient (D_0) both show a slight decreasing, then rapid increasing trend. The D_0 of five coals jumps at R_o = 1.26%. V_L increases alongside that of the micropores volume. Similarly, the methane desorption capacity in the first minute increases slowly at first and then rapidly as the micropores volume increase. With the decrease of the Raman parameter I_{D1}/I_G, the V_L, methane desorption volume within 7200 s and D_0 all increase. Results show that coalification changes the microporous structure and the macromolecular structure of the coal, which finally affects the diffusion capacity of coal. Coalification has a positive effect for the gas extraction and the development of CBM for the semianthracites.

Keywords: coalification; molecular structure; desorption; gas diffusion; time-dependent; Raman parameter

1 Introduction

Coal mining depth in China are increasing at a rate of 10 to 20 meters per year with some of these are even up to 20 to 40 meters per year. With increases in mining depth, the temperature of coal seam also increases. An increase in temperature with burial depth is certainly a significant factor in coal metamorphism (Hower and Gayer, 2002). In these conditions coal has a tendency towards a higher degree of coalification. And the low and middle rank coals may change into middle-high rank coals (MHRC) (Jiang et al., 2019a). For the deep-buried coals, they are characterized by high gas pressure and high geostress. Under these conditions, coal and gas outbursts disaster is more like to happen induced by mining. Meanwhile, the coalbed methane (CBM) drainage also face huge challenges (Cheng et al., 2011; Jiang et al., 2015). In order to extract CBM efficiently, it is necessary to

understand both the methane adsorption capacity and the diffusion dynamics of deep-buried coal reservoirs in middle and high rank.

Coalification is a complex forming process of coal body after decomposition of vegetal matter, and the coalification jump leads to sudden changes in the physicochemical properties and pore structure of coal (Liu et al., 2018b; Jiang et al., 2019a). With the development of coal mineralization, there may be jumps of four to five times in coalification during the structural evolution of coal (Bustin and Guo, 1999; Tao et al., 2018; Li et al., 2016a; Zhou et al., 2017). Studies indicate that coalification (jumps) causes dramatic changes in the behavior of gas desorption and diffusion in coal (Laxminarayana and Crosdale 1999; Hildenbrand et al., 2006; Zhang et al., 2011; Merkel et al., 2015; Cheng et al., 2017). Coalification leads to pore structure of coal more complex, especially for the micropores and transition pores (Wang et al., 2015). One computational scheme has been developed based on the data of high-pressure sorption isotherms and desorption data from two Central European coal basins; the maximum CBM sorption capacity of coal can be calculated out, as a function of coal rank, pressure and temperature (Hildenbrand et al., 2006). With the increase of the degree of coalification, the micropores volume, ultimate desorption volume and initial diffusion coefficient of the four coal samples in northern China tended to decrease first from lignite to high-volatility bituminous (R_o=0.64%) and then increase from high-volatility bituminous to midium-volatility bituminous/anthracite (Guo et al., 2016a). Therefore, it is of great significance to study the effect of coalification on methane desorption and diffusion behavior in coals.

In addition, the behavior of methane diffusion in coal particle is affected by desorption equilibrium pressure, the deformation degree of coal caused by the tectonic movement, coal particle size and moisture content (Busch and Gensterblum, 2011; Pan et al., 2010; Tang et al., 2015; Dong et al., 2017; Cheng et al., 2017; Yue et al., 2017; Cheng and Pan, 2019). Previous studies show that the diffusion of gas in the coal matrix is much slower than the classic Darcy's flow (Liu and Lin, 2019; Zhao et al., 2017). To simplify calculation in the model, diffusion effects are not usually be considered; Fracture permeability is used in this place to describe the whole process of gas extraction (Pan and Connell, 2012). However, ignoring the diffusion effect may be lead to the calculation result of the flow permeability larger than the true value (Zhao et al., 2019). The effective diffusion coefficient of high

and low rank coal increase logarithmically with the increase of the gas pressure. However, the effective diffusion coefficient of high rank coal is smaller than that of low rank coal (Meng and Li, 2018).

In past decades, scholars have proposed several different diffusion models including the widely used unipore diffusion model, the bidisperse diffusion as well as the fractional diffusion model (Guo et al., 2016b; Yue et al., 2017; Liu and Lin, 2019; Zhao et al., 2019). These models are based on Fick's diffusion theory, which assumes a constant diffusion coefficient. However, the gas diffusion coefficient of coal particle shows the characteristic phenomenon of decreasing with time. Classical diffusion models with a constant diffusion coefficient are inadequate in describing the behavior of diffusion in coal over the entire desorption timescale (Li et al., 2016b; Zhao et al., 2017). It is effective to treat Fick's diffusion coefficient as a variable physical quantity (Latour et al., 1993; Valiullin and Skirda, 2001; Dong et al., 2017). Latour et al. (Latour et al., 1993) began studying time-dependent diffusion coefficients of fluids in porous media as early as 1993. Then, the Monte Carlo autocorrelation function was used to simulate time-dependent self-diffusion coefficient of porous media (Valiullin and Skirda, 2001). Some scholars proposed several new multi-scale dynamic diffusion models, as a new method for calculating accurate desorption characteristics as for the process in whole time scale. These models can better calculate gas content and outburst prediction indexes (Li et al., 2015; Li et al., 2016b; Zhao et al., 2017; Liu and Lin, 2019). Common feature of these diffusion models is the time-dependent diffusion coefficient.

In this work, the behavior of methane diffusion in five coal samples of MHRC was studied. Based on the relationship between diffusion coefficient and time, a multi-scale pores diffusion model was introduced. In addition, the microporous properties and Raman parameters also were used to study the influence of coalification on methane diffusion behavior in coal.

2 Coal samples and experiment methods

2.1 Coal samples

Five MHRC samples were sampled from sites as follows; the Daxing Coal Mine of Liaoning Province, Shuangliu Mine of Shanxi Province, Yangliu Mine of Anhui Province, Sijiazhuang Mine of Shanxi Province and Wolonghu Mine of Anhui province. The location map of these coal mines are shown in

Fig. 1. Table 1 shows the results of proximate analysis, element, R_o and Raman parameter I_{D1}/I_G.

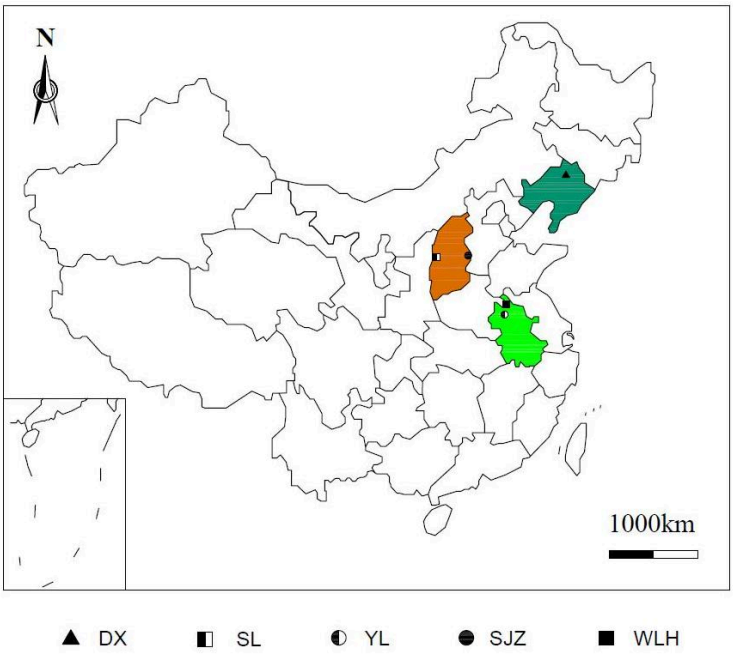

Fig. 1 Map showing coal mines and samples locations. DX, Daxing Mine in Liaoning Province; SL, Shuangliu Mine in Shanxi Province; YL, Yangliu Mine in Anhui Province; SJZ, Sijiazhuang Mine in Shanxi Province; WLH, Wolonghu Mine in Anhui province.

Table 1. The results of proximate analysis, element, R_o and Raman parameter I_{D1}/I_G (Jiang et al., 2019b)

Sample	Proximate analysis (wt.%)				Ultimate analysis (wt.%)			R_o (%)	Coal rank	I_{D1}/I_G (cm^{-1})
	M	A	VM	FC	C	H	O			
DX	5.90	10.13	34.14	49.83	77.94	6.24	13.93	0.66	hvb	1.24
SL	0.89	30.70	19.01	49.40	84.83	5.74	7.43	1.21	lvb	1.20
YL	0.50	7.40	30.63	61.47	86.35	5.66	5.92	1.26	mvb	1.22
SJZ	3.18	10.13	8.45	78.24	89.98	3.65	3.46	2.63	sa	0.89
WLH	4.75	13.54	9.53	72.18	90.93	2.45	4.89	3.18	sa	0.75

M: moisture; A: ash, on a dry basis; VM: volatile matter, on dry ash free (daf) basis; FC: fixed carbon (daf basis); all ultimate analyses reported on a daf basis except sulfur on a dry basis; C: carbon content; H: hydrogen content; O: oxygen content; R_o: mean random vitrinite reflectance (%, oil); Coal rank is determined according to ASTM D388-2015. hvb: high volatile bituminous; mvb: middle volatile bituminous; lvb: low volatile bituminous; sa: semianthracite; I_{D1}/I_G: intensity ratio of the D peak and the G peak.

2.2 Experimental method

2.2.1 Scanning electron microscopy

Scanning electron microscopy (SEM) experiments were carried out on five MHRC samples using FEI Quanta TM 250 (USA). According to the standard of GB/T 20307-2006, the coal samples were cut into approximately cube with size of 10 mm ×10 mm ×10 mm. During the sample preparation process, make sure that the samples were dried, not polluted as well as the surface to be observed were not

damaged. Then, to increase the conductivity of sample, ion sputtering technology was used to plate gold on coal surface, and the thickness of the gold-plating layer s controlled at 5 ~ 10 nm.

2.2.2 Methane isothermal adsorption test

The high-pressure methane adsorption isotherms were measured following the MT/T 752-1997 Standard, using HCA high-pressure volumetric equipment (Chongqing Research Institute of CCTEG, China). Firstly, about 50 g of coal sample with particle size of 0.2~0.25 mm was placed in a vacuum drying oven. After drying under 4 Pa /100 °C for 2.5 h, the sample was placed to room temperature and put in a sample container for an evacuation under 4 Pa at 60 °C for 24 h. After the evacuation, the sample container was cooled to 30 °C and the dead space volume in the container was determined by helium gas. Then, evacuation was applied to completely exhaust the residual helium for 2 h. The methane adsorption isotherm was tested at 30 °C with a maximum gas pressure of 4.00 MPa by the volumetric method. The sample container was linked to a reference container with measured dead volume. In the same way, the volume changes of free gas in the sample container could be obtained by the pressure changes when the adsorption was balanced. Finally, the adsorption volume can be calculated by subtracting the free volume from the entered methane volume (Jin et al., 2016). The measured adsorption isotherm were on dry ash-free (daf) basis.

2.2.3 Methane desorption test

Firstly, approximately 50 g of the coal sample (were crushed to a particle size of 0.2~0.25 mm) was placed into the sample container for degassing. And it experienced an evacuation under 4 Pa at 60 °C for 24 h, completely removing the impurities in coal. Then, the container was injected with methane and put in a 30 °C water bath for gas adsorption. Equilibrium pressures in methane desorption tests were: 0.74 MPa, 1.00 MPa, 2.00 MPa, 3.00 MPa and 4.00 MPa, and the cumulative desorption time for each coal particle was 7200 seconds (s). When adsorption equilibrium was achieved, opened the container and connected it to the gas volume measuring cylinder. The volume of gas desorbed from the sample at different times (intervals of 20 s read once) was read and recorded from the cylinder (Jin et al., 2016). The adsorption equilibrium/desorption experimental setup is shown in Fig. 2.

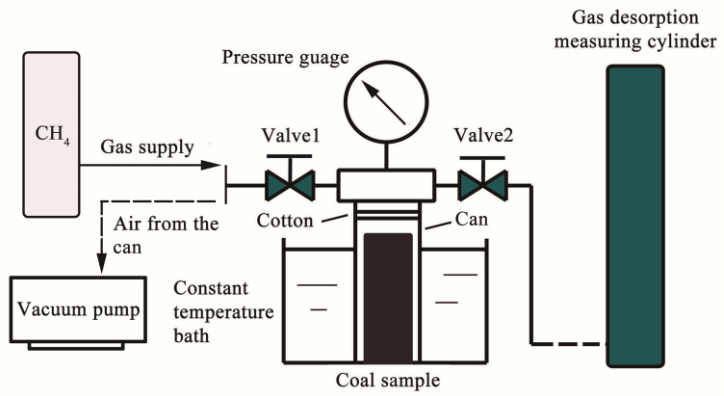

Fig. 2 Adsorption equilibrium/desorption experimental setup

2.2.4 Apparent density of coal test

Under the room temperature of 20 °C, the coal sample with particle size of 1~3 mm was weighed and then coated with wax on their surface. After that, put the wax-coated coal particles into a density bottle and using the sodium dodecyl sulfate solution as the wetting agent to measure the volume of solution displaced by the wax-coated coal particles (namely the apparent volume of wax-coated coal). Thus, the apparent density of the wax-coated coal particles could be calculated, and the apparent density of coal could also be calculated by subtracting the density of wax.

2.2.5 Calculation of methane diffusion coefficient

Based on the experimental phenomenon that both the coefficients of gas diffusion decaying with time and the diffusion mechanism of gas in multi-scale pores of coal are associated. The physical model of the multi-scale pores was introduced in the previous work (Li et al., 2016b); here the assumption is that there is a negative exponential function between the diffusion coefficient and time. This is shown in Eq. (1) (Li et al., 2015; Li et al., 2016b).

$$D(t) = D_0 exp(-\beta t) \qquad (1)$$

Where D(t) is the time-dependent diffusion coefficient, mL/g; D_0 is the initial diffusion coefficient at t = 0, mL/g; β is the attenuation coefficient of the diffusion coefficient, s^{-1}.

When gas diffuses, it first begins to diffuse from the small pores with less resistance. Over time, the diffusion gradually develops towards smaller pores. The diffusion resistance changes from small to large and the diffusion coefficient changes from large to small with time (Li et al., 2015). Based on the above, the gas diffusivity can be obtained, which is a new diffusion model, as shown in Eq. (2) (Li et al.,

2016b).

$$\frac{Q_t}{Q_\infty} = 1 - \frac{6}{\pi^2}\sum_{n=1}^{\infty}\frac{1}{n^2}exp\left(-\frac{n^2\pi^2 D_0}{r_0^2\beta}\left(1-e^{-\beta t}\right)\right) \quad (2)$$

Where Q_t is the cumulative volume of diffusion at time t, mL/g; Q_∞ is the ultimate diffusion amount, mL/g; $\frac{Q_t}{Q_\infty}$ is the cumulative diffusivity at time t; D_0 is the initial diffusion coefficient; r_0 is the particle radius, cm; Q is the initial total gas content, which is calculated according to Eq. (3) (Li et al., 2016b).

$$Q = \frac{abp}{1+bp}\frac{100-A-M}{100}\frac{1}{1+0.31M} + \frac{10P\varphi 273}{\rho(273+t_w)} \quad (3)$$

Where Q is the initial total gas content, cm^3/g; a, b is the adsorption constant; P is the adsorption equilibrium pressure, MPa; A is the ash, %; M is the moisture, %; ϕ is the porosity, %; ρ is the apparent density, g/cm^3; t_w is the temperature of water bath, °C. The Q_∞ can be calculated according to Eq. (4).

$$Q_\infty = Q - Q_t \quad (4)$$

Based on the above diffusion theory and laboratory data, the D_0 and β can be obtained by fitting the desorption data using the MATLAB software. Finally, the D_t and its relation with time is obtained.

3 Results and discussion

3.1 Effect of coalification on methane adsorption characteristics of coal particle

The results of SEM of five coal samples is shown in Fig. 3.

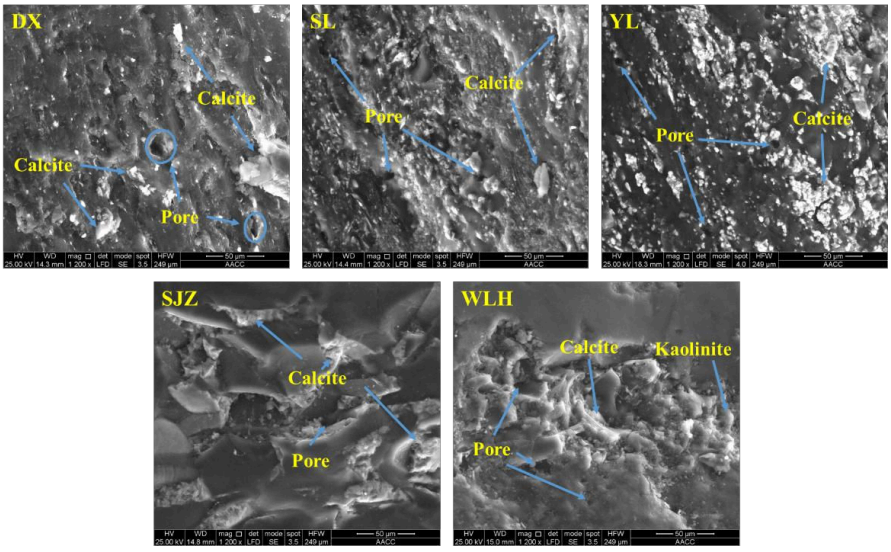

Fig. 3 SEM result of middle-high rank coal samples

Many pore structures and minerals (calcite and kaolinite) were observed in Fig. 3. The surface morphology of the five different metamorphic coal samples varied greatly. The SJZ and WLH coal

samples are rougher than the DX, SL and YL coal samples, indicating that the pore structure of the coal surface with higher metamorphism is more complicated (Fig. 3). Cylindrical pores were found in DX, SL and YL, and surface mylonization was found in WLH coal sample, which may be due to tectonic movement and coal mineralization. The SEM image helps to characterize the pore structure of the coal surface (Liu et al., 2018). Complex pore structures in coal matrices provide channels and spaces for gas adsorption/desorption (Han et al., 2013).

The results of methane isothermal adsorption experiments of five samples are shown in Table 2.

Table 2. Langmuir volume, apparent density, porosity and micropores volume of five coal samples

Coal sample	DX	SL	YL	SJZ	WLH
Langmuir volume (V_L) (m^3/t)	25.13	21.03	17.24	50.00	47.65
Langmuir pressure (P_L) (MPa^{-1})	0.42	0.54	1.37	1.03	0.75
Apparent density (g/cm^3)	1.13	1.05	0.77	1.04	0.80
Porosity (%)	4.8623	2.6403	2.0709	4.6788	1.5774
Micropore volume (mL/g)	0.0640	0.0300	0.0420	0.0860	0.0970

Note: Porosity and micropore (pores < 2nm) volume data are cited from previous work (Jiang et al., 2019a).

The V_L for daf basis of coal samples DX, SL and YL, SJZ, WLH were 25.13 m^3/t, 21.03 m^3/t, 17.24 m^3/t, 50.00 m^3/t and 47.65 m^3/t, respectively. The order of adsorption capacity from large to small is SJZ > WLH > DX > SL > YL. The methane adsorption isotherms are shown in Fig. 4.

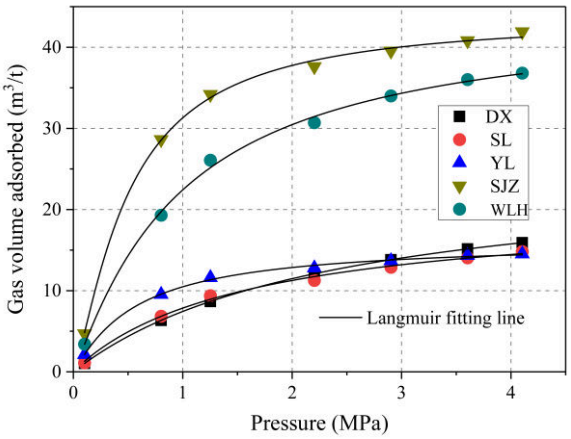

Fig. 4 CH_4 adsorption isothermal of five coal samples

Under the different gas pressures, the isothermal adsorption curves of five different metamorphic coal samples are conform to the Langmuir equation. With increases in the equilibrium gas pressure, the gas adsorption volume gradually increases, though the overall rate decreases (Figure 4). From the adsorption curve, the initial desorption rate and V_L of semianthracites samples SJZ and WLH were obviously larger than samples YL, SL and DX.

The relationship between the R_o and V_L of the five coal samples are shown in Fig. 5.

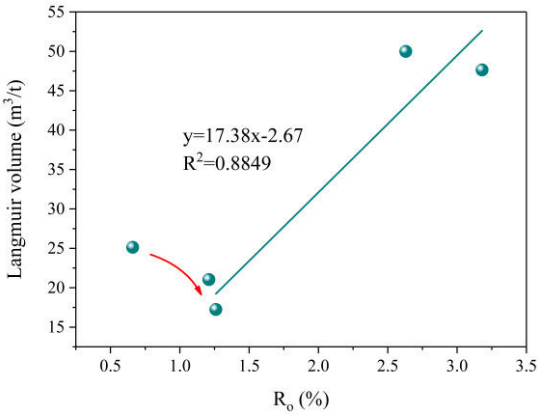

Fig. 5 Relationship between vitrinite reflectance (R_o) and Langmuir volume

It can be seen from Fig. 5 that when R_o < 1.26%, the V_L for daf basis of the sample decreases with the increase of R_o from 25.13 m^3/t to 12.24 m^3/t. However, When R_o > 1.26%, the V_L of the coal sample increases with the increase of R_o from 12.24 m^3/t to 50.00 m^3/t. When R_o > 3.00%, the V_L slightly decreases to 47.65 m^3/t. The V_L for daf basis of the subbituminous and bituminous coals from Northeast China changes from 20.07 m^3/t to 25.8 m^3/t, indicating that these coals have moderate to large methane adsorption capacity (Cai et al., 2013).

3.2 Influence of coalification on methane diffusion kinetics of coal

3.2.1 Methane desorption capacity of coal particles

The relationships between the cumulative CH_4 desorption volume and time in 7200 s for five coal samples are shown in Fig. 6.

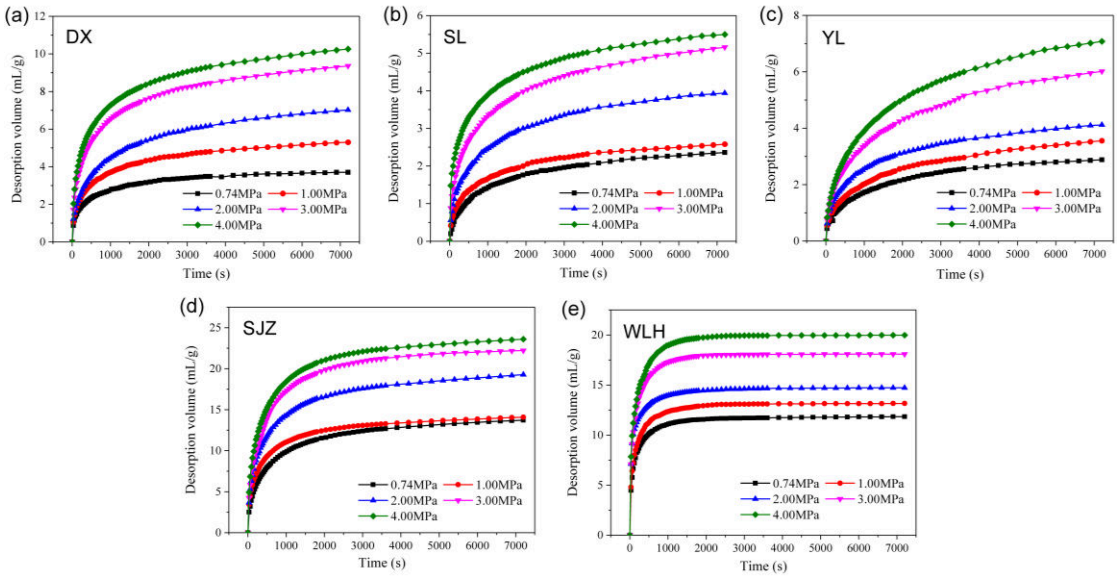

Fig. 6 Relationships between methane desorption volume and time under different gas pressures

Taking the equilibrium pressure of 4.00 MPa as an example, the maximum desorption volume of DX, SL, YL, SJZ and WLH samples within 7200 s was 10.26 mL/g, 5.50 mL/ g, 7.08 mL/g, 23.60 mL/g, and 19.98 mL/g. The cumulative gas desorption volumes of semianthracites samples SJZ and WLH are significantly larger than that of the DX, SL and YL (Fig. 6). The order of cumulative gas desorption volume of coal samples in 7200 s is SJZ > WLH > DX > YL > SL (Fig. 6), which indicates that high rank coals SJZ and WLH may contain abundant open micropores (Fig. 3). In addition, the proportion of gas desorption volume in the first 600 s (divide total gas desorption volume within 7200 s) was 55%, 63%, 45%, 68% and 89%, respectively. The semianthracites sample WLH, which has a maximum values of R_o = 3.18%, accounted for the largest initial desorption rate.

In order to study the effect of coalification on the desorption characteristics of coals in different desorption period, the relationships between R_o and the cumulative desorption volumes in the first minute (Q_{1min}), in the first three minutes (Q_{3min}) and in the 120 minutes (Q_{120min}) were analyzed. The relationships between gas desorption volume (Q_{1min}, Q_{3min}, and Q_{120min}) and R_o are shown in Fig. 7.

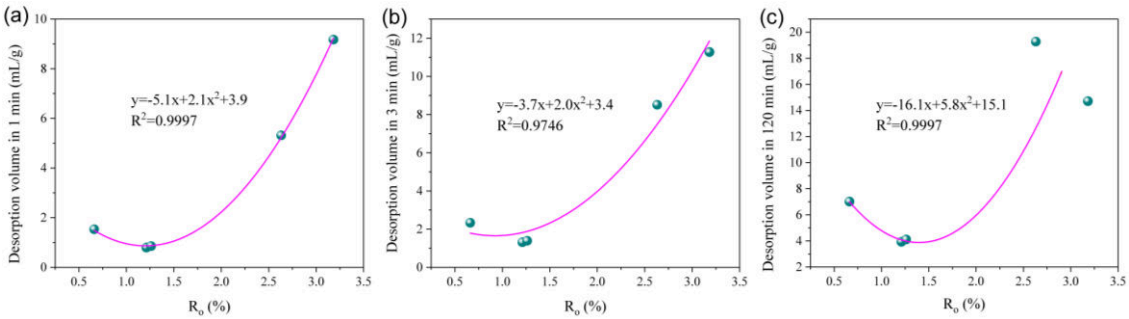

Fig. 7 Relationships between cumulative desorption volume in 1min (a), 3min (b) and 120min (c) (Q_{1min}, Q_{3min}, and Q_{120min}) and R_o under gas pressure of 2.00 MPa

It can be seen from Fig. 7 that, with the increase of R_o, the cumulative desorption volume of gas desorption (Q_{1min}, Q_{3min} and Q_{120min}) have a tendency of decrease from high volatile bituminous to medium/low volatile bituminous and an increase starting low volatile bituminous to semianthracites. When R_o < 1.26%, the desorption volume in 1min (Q_{1min}) of coal sample decreased from 1.54 mL/g to 0.80 mL/g. However, When R_o > 1.26%, the desorption volume in one min increases from 0.80 mL/g to 9.18 mL/g (Fig. 7a). The gas desorption volume (Q_{1min}, Q_{3min}, and Q_{120min}) of five coals jumps at R_o = 1.26%, which was defined as the third jump in previous work (Jiang et al., 2019a). As the

semianthracites (SJZ and WLH) can desorb more gas than middle rank coals (DX, SL and YL), once the desorption gas dynamic equilibrium of coal is broken, e.g. affected by coal mining, SJZ and WLH coals are more likely to have gas abnormal effusing or gas outburst accidents. This indicates that semianthracite coals SJZ and WLH usually have a higher desorption capacity.

3.2.2 Time-dependent methane diffusion coefficient of coal particle

According to Eq. (1), MATLAB software was used to fit the methane desorption data of five kinds of MHRC. The fitting curve under gas pressure on 2.00 MPa is taken as an example. Figure 8 shows the relationship between methane diffusivity and the time t.

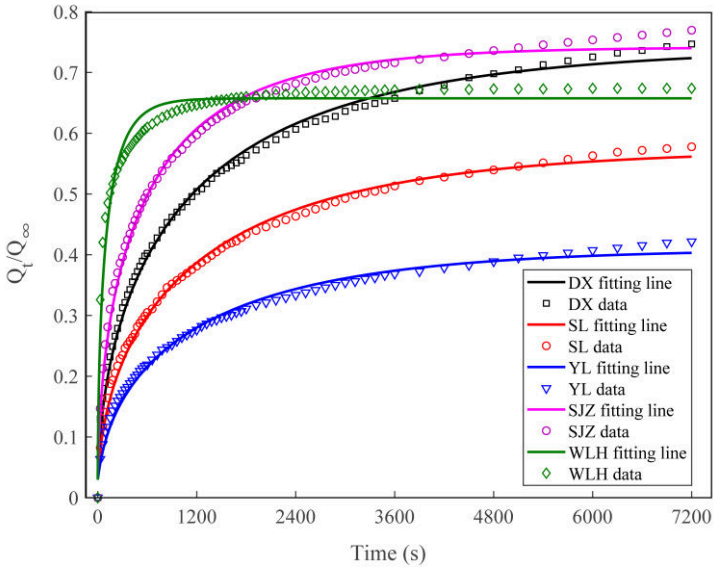

Fig. 8 Relationship between methane diffusivity (Q_t/Q_∞) and time (second) under gas pressure of 2.00 MPa (Q_t is desorption volume at time t, Q_∞ is ultimate desorption volume)

The initial diffusion coefficient (D_0) and diffusion coefficient (β) fitting results of the five coal samples under different gas pressures are listed in Table 3.

Table 3. Initial diffusion coefficient (D_0) and attenuation coefficient (β) of five coal samples

Coal sample	0.74 MPa		1.00 MPa		2.00 MPa		3.00 MPa		4.00 MPa	
	D_0 ($10^{-8}m^2/s$)	β ($10^{-2}s^{-1}$)	D_0 ($10^{-8}m^2/s$)	β ($10^{-2}s^{-1}$)	D_0 ($10^{-8}m^2/s$)	β ($10^{-2}s^{-1}$)	D_0 ($10^{-8}m^2/s$)	β ($10^{-2}s^{-1}$)	D_0 ($10^{-8}m^2/s$)	β ($10^{-2}s^{-1}$)
DX	2.41	4.13	2.31	2.70	1.00	2.22	1.62	3.18	1.64	3.74
SL	0.67	1.69	0.65	2.93	0.53	2.44	0.71	2.83	0.97	4.73
YL	0.30	2.14	0.29	2.00	0.27	2.77	0.35	1.58	0.41	1.29
SJZ	2.23	2.55	2.27	5.41	1.87	4.17	1.83	4.12	1.98	4.86
WLH	12.37	6.52	9.39	11.24	7.67	24.38	5.97	15.90	5.60	14.48

The D_0 of coal samples of DX, SL, YL, SJZ and WLH under gas pressure of 2.00 MPa are 1.00×10^{-8} m^2/s、0.53×10^{-8} m^2/s、0.27×10^{-8} m^2/s、1.87×10^{-8} m^2/s and 7.67×10^{-8} m^2/s, respectively (Table 3). Fitting

accuracy (R^2) are 0.9982, 0.9978, 0.9960, 0.9976, and 0.9795, respectively. Moreover, similar changes were observed under other pressures. Indicate that Eq. (1) can describe the methane full-time diffusion behavior in coal accurately. For five coal samples, the D_0 decreases with time going on. Semianthracites coal WLH has the largest D_0, followed by SJZ, DX and SL, and the minimum is YL.

Figure 9 shows the relationship between initial diffusion coefficient (D_0) and R_o of five coal samples under different gas pressures.

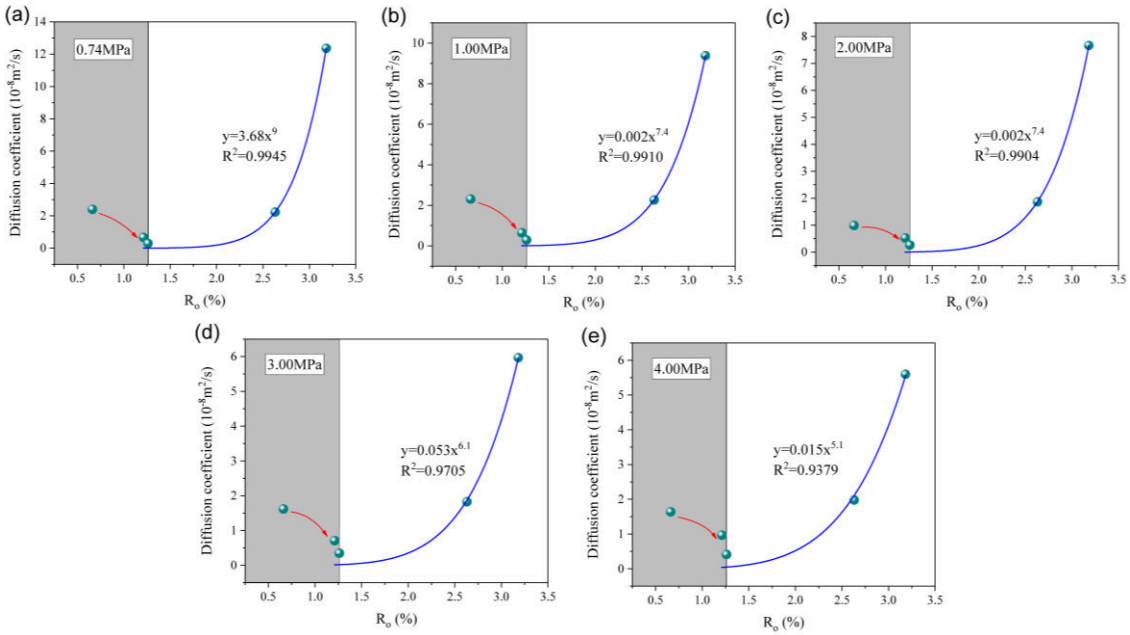

Fig. 9 Relationship between initial diffusion coefficient (D_0) and R_o of five coals under different gas pressures

With the increase of R_o, the initial diffusion coefficient of coal has a tendency of a decrease from high volatile bituminous to medium/low volatile bituminous and an increase starting low volatile bituminous to semianthracites (Fig. 9). D_0 of five coals jumps at R_o = 1.26%, which was defined as the third jump in previous work (Jiang et al., 2019a). When R_o < 1.26%, D_0 gradually decreases with the increase of R_o. While R_o > 1.26%, D_0 increases with the increase of R_o. It indicates that the gas diffusion capacity of coal decrease from high volatile bituminous to medium/low volatile bituminous and an increase starting low volatile bituminous to semianthracites with the improving of coal rank.

The coalification processes causing the parabolic relationships and nonlinear behavior of the gas desorption volume and D_0 with coal rank transitioning from high volatile bituminous to semianthracite (see Fig. 7 and Fig. 9) was mainly due to the third coal coalification jump. As the third coalification

jump has a turning effect on the micropores development (Jiang et al., 2019a). The micropores of coal matrix determine the gas desorption and diffusion capacity in coal.

3.3 Effects of micropores on diffusion behavior of coal

The pore structure of coal, especially the micropores volume (pore diameter < 2 nm), determines the gas adsorption capacity of coal (Clarkson and Bustin, 1999; Cai et al., 2013; Nie et al., 2015; Wang et al., 2014). The micropores volume obtained by CO_2 adsorption (Jiang et al., 2019a) are listed in Table 2. Figure 10 shows the relationships between the micropores volume and V_L, the cumulative CH_4 desorption volume in 60 s, the cumulative desorption volume in 7200 s, and the initial diffusion coefficient D_0 under gas pressure of 2.00 MPa.

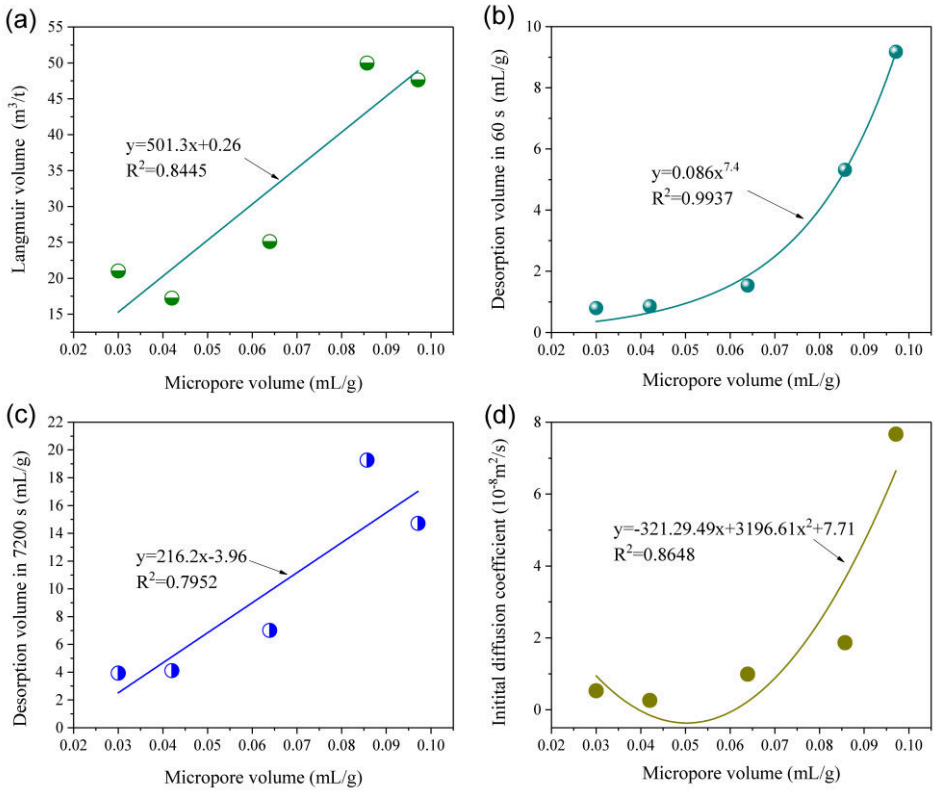

Fig. 10 Relationship between micropores volume and V_L (a), CH_4 desorption volume in 60 seconds (b), desorption volume in 7200 seconds (c), and initial diffusion coefficient D_0 under gas pressure of 2.00 MPa (d).

With the increase of the microspores volume, V_L tends to increase generally follows a linear relationship (Fig. 10a). It indicates that, the larger the micropores volume of the coal, the stronger the methane adsorption capacity. The cumulative desorption volume in 60 s enlarges with the increase of

the micropores volume, showing a power function relationship (Fig. 10b). Imply for the desorbed volume increase rapidly the in initial short time. However, see from the full-time desorption, with the increase of the micropores volume, the cumulative desorbed volume tends to increase follows a linear relationship in 7200s (Fig. 10c). In addition, the microspores structure of the coal matrix highly effective the diffusion behavior. With the increase of the microspores volume, D_0 (under gas pressure of 2.00 MPa, Table 3) tends to decrease slightly from high volatile bituminous to medium/low volatile bituminous and an increase continuously starting low volatile bituminous to semianthracites follows a parabolic relationship (Fig. 10d). The relationship curve between microspores volume and D_0 is approximately u-shaped.

3.4 Effect of Raman parameters of coal on desorption/diffusion behavior

The Raman spectroscopy such as peak position difference (G-D1), position of G and D1 peaks, and intensity ratio of the D peak and the G peak (ID1/IG) are applied to evaluate the defect in carbonaceous materials or degree of crystallinity (Schwan et al., 1996; Smith et al., 2016). Raman parameters especially I_{D1}/I_G can reflect changes in the macromolecular structure of the coal (Li et al., 2012; Jiang et al., 2019b). The Raman parameter I_{D1}/I_G is a good indicator for evaluating coal ranks because it has a better correlation with R_o (Li et al., 2006). The relationship between Raman characteristic parameters I_{D1}/I_G and R_o of five samples of MHRC is a linear function ($y = -0.2x + 1.43$, $R^2 = 0.9549$) (Jiang et al., 2019b).

The analysis of the relationship between Raman parameter I_{D1}/I_G and micropores volume, adsorption/desorption capacity, and diffusion coefficient is of great significance to reveal the internal relationship between the microscopic characteristics of the molecular structure of coal and the gas diffusion behavior. The relationship between the Raman parameter I_{D1}/I_G (intensity ratio of the D peak and the G peak) (Table 1), micropores volume, V_L, gas desorption volume within 7200 s and D_0 (under the gas pressure of 2.00 MPa) is shown in Fig. 11.

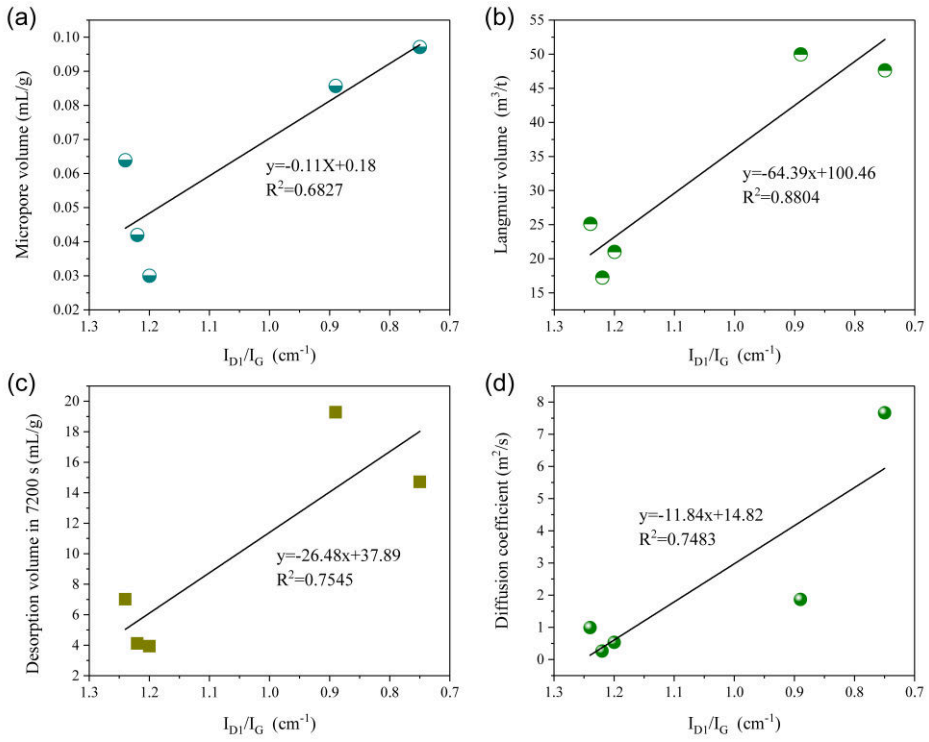

Fig. 11 Relationship between the Raman parameter (I_{D1}/I_G, intensity ratio of the D peak and the G peak), and micropores volume (a), V_L (b), gas desorption volume within 7200 seconds (c) and D_0 (d)

As the I_{D1}/I_G decreases from 1.24cm^{-1} to 0.75cm^{-1}, the micropores volume increases from 0.030 mL/g to 0.097 mL/g (Fig. 11a). The V_L, cumulative desorption volumes in 7200 s and the D_0 also showed the same trends. The V_L increases from 17.24 m^3/t to 50.00 m^3/t (Fig. 11b), the cumulative desorption volumes in 7200 s increases from 3.94 mL/g to 19.28 mL/g (Fig. 11c), while the D_0 (under the gas pressure of 2.00 MPa) increases from a minimum of 0.27 × 10^{-8} m^2/s to 7.67 × 10^{-8} m^2/s (Fig. 11d). It indicates that the adsorption/desorption and diffusion capacities of the five coals all increase with the decrease of I_{D1}/I_G.

As coalification improves, the I_{D1}/I_G of the five middle-high rank coal samples decreases, and the coal structure develops towards graphitization, indicating the degree of ordering of the molecular structure increases, further affects the complexity of the pores and the adsorption and desorption characteristics in the coals (Sadezky et al., 2005). The coal molecular structure determines the coal porosity and evolution of micropores. In different stages of coalification, the porosity and evolution of micropores are determined by the different functional groups of coal (Liu et al., 2018b).

The research results indicate that under the conditions of deep mining, the coalification may leads

to the development of micropores in the semianthracite (SJZ and WLH) and the improvement of gas diffusion capacity, which is positive to the gas extraction and the development of CBM. Whether the micropore structure or the functional group of the coal macromolecular structure determines the gas desorption and diffusion capacity of the coal still needs further investigation.

4 Conclusions

In this paper, the effects of coalification on coal adsorption, desorption and diffusion behavior for five samples of MHRC were studied. The main conclusions are as follows:

(1) Overall, the CH_4 adsorption capacity for coalification is enhanced. As the R_o increased, the V_L increased from 17.24 mL/g to 50.00 mL/g. The order of adsorption capacity from large to small was SJZ > WLH > DX > SL > YL. With increases in the R_o, the cumulative desorption volume showed a trend of decrease from high volatile bituminous to medium/low volatile bituminous and an increase starting from low volatile bituminous to semianthracites. When R_o < 1.26%, the desorption volume decreased from 1.54 mL/g to 0.80 mL/g. When R_o >1.26%, the desorption volume increased from 0.80 mL/g to 9.18 mL/g.

(2) Coalification especially for the third coalification jump (R_o = 1.26%) showed a turning effect on diffusion dynamics of MHRC. With the increase of R_o, the D_0 of coal particles has a tendency of a decrease from high volatile bituminous to medium/low volatile bituminous and then an increase starting from low volatile bituminous to semianthracites. D_0 of five coals jumps at R_o = 1.26%. When R_o < 1.26%, D_0 gradually decreases with the increase of R_o. However, while R_o > 1.26%, D_0 increases with the increase of R_o.

(3) The microspores structure of the coal matrix highly effective the diffusion behavior. With the increase of the micropores volume, in general V_L tends to increase, the cumulative desorbed volume tends to increase follows a linear relationship in 7200s, D_0 tends to decrease slightly from high volatile bituminous to medium/low volatile bituminous and an increase continuously starting low volatile bituminous to semianthracites. The relationship curve of micropores volume and D_0 is approximately u-shaped. The Raman parameter (I_{D1}/I_G) has a significant effect on the gas diffusion behavior. The V_L, cumulative desorption volume and D_0 are negatively correlated with the I_{D1}/I_G as a whole, and all increase with the decrease of the I_{D1}/I_G.

(4) The research results indicate that under the conditions of deep mining, the coalification may leads to the development of micropores in the semianthracites (SJZ and WLH) and the improvement of gas diffusion capacity, which is a positive factor for the gas extraction and the development of CBM.

Notes

The authors declare that we do not have any commercial or associative interest that represents a conflict of interest in connection with the work submitted.

Acknowledgements

The authors are grateful to the Fundamental Research Funds for the National Natural Science Foundation of China (No. 51874298; No. 51804201) and the Priority Academic Program Development of Jiangsu Higher Education Institutions (PAPD).

References

Busch, A., Gensterblum, Y., 2011. CBM and CO_2-ECBM related sorption processes in coal: A review. Int. J. Coal Geol. 87, 49-71.

Bustin, R.M., Guo, Y., 1999. Abrupt changes (jumps) in reflectance values and chemical compositions of artificial charcoals and inertinite in coals. Int. J. Coal Geol. 38, 237-260.

Cai, Y.D., Liu, D.M., Pan, Z.J., Yao, Y.J., Li, J.Q., Qiu, Y.K., 2013. Pore structure and its impact on CH_4 adsorption capacity and flow capability of bituminous and subbituminous coals from Northeast China. Fuel. 103, 258-268.

Clarkson, C.R., Bustin, R.M., 1999. The effect of pore structure and gas pressure upon the transport properties of coal: a laboratory and modeling study. 1. Isotherms and pore volume distributions. Fuel. 78, 1333-1344.

Cheng, Y.P., Jiang, H.N., Zhang, X.L., Cui, J.Q., Song, C., Li, X.L., 2017. Effects of coal rank on physicochemical properties of coal and on methane adsorption. Int. J. Coal Sci. Technol. 4, 129-146.

Cheng, Y.P., Pan, Z.J., 2020. Reservoir properties of Chinese tectonic coal: A review. Fuel. 260, 116350.

Cheng, Y.P., Wang, L., Zhang, X.L., 2011. Environmental impact of coal mine methane emissions and responding strategies in China. Int. J. Greenhouse Gas Control. 5, 157-166.

Chen, S.J., Jin, L.Z., Chen, X.X., 2011. The effect and prediction of temperature on adsorption capability of coal/CH_4. Procedia Eng. 26, 126-131.

Clarkson, C.R. Bustin, R.M., 1999. The effect of pore structure and gas pressure upon the transport properties of coal: a laboratory and modeling study. 2. Adsorption rate modeling. Fuel. 78, 1345-1362.

Dong, J., Cheng, Y., Liu, Q., Zhang, H., Zhang, K., Hu, B., 2017. Apparent and True Diffusion Coefficients of Methane in Coal and Their Relationships with Methane Desorption Capacity. Energy Fuels. 31, 2643-2651.

Guo, H.J., Cheng, Y.P., Ren, T., Wang, L., Yuan, L., Jiang, H.N., Liu, H.Y., 2016a. Pulverization

characteristics of coal from a strong outburst-prone coal seam and their impact on gas desorption and diffusion properties. J. Nat. Gas Sci. Eng. 33, 867-878.

Guo, H.J., Cheng, Y.P., Yuan, L., Wang, L., Zhou, H.G., 2016b. Unsteady-State Diffusion of Gas in Coals and Its Relationship with Coal Pore Structure. Energy Fuels. 30, 7014-7024.

Han, F.S., Busch, A., Krooss, B.M., Liu, Z.Y., Yang, J.L., 2013. CH_4 and CO_2 sorption isotherms and kinetics for different size fractions of two coals. Fuel. 108, 137-142.

Hildenbrand, A., Krooss, B.M., Busch, A., Gaschnitz, R., 2006. Evolution of methane sorption capacity of coal seams as a function of burial history-a case study from the Campine Basin, NE Belgium. Int. J. Coal Geol. 66, 179-203.

Hower, J.C., Gayer, R.A., 2002. Mechanisms of coal metamorphism: case studies from Paleozoic coalfields. Int. J. Coal Geol. 50, 215-245.

Jiang, J.Y., Cheng, Y.P., Zhang, P., Jin, K., Cui, J., Du, H., 2015. CBM drainage engineering challenges and the technology of mining protective coal seam in the Dalong Mine, Tiefa Basin, China. J. Nat. Gas Sci. Eng. 24, 412-424.

Jiang, J.Y., Zhang, Q., Cheng, Y.P., Jin, K., Zhao, W., Guo, H., 2016. Influence of thermal metamorphism on CBM reservoir characteristics of low-rank bituminous coal. J. Nat. Gas Sci. Eng. 36, 916–930.

Jiang, J.Y., Yang, W.H., Cheng Y.P., Zhao, K., Zheng, S.J., 2019a. Pore structure characterization of coal particles via MIP, N_2 and CO_2 adsorption: Effect of coalification on nanopores evolution. Power Technology. 354, 136-148.

Jiang, J.Y., Yang, W.H., Cheng, Y.P., Liu, Z.D., Zhang, Q., Zhao, K., 2019b. Molecular structure characterization of middle-high rank coal via XRD, Raman and FTIR spectroscopy: Implications for coalification. Fuel. 239, 559-572.

Jin, K., Cheng, Y.P., Liu, Q.Q., Zhao, W., Wang, L., Wang, F., Wu, D.M., 2016. Experimental Investigation of Pore Structure Damage in Pulverized Coal: Implications for Methane Adsorption and Diffusion Characteristics

Latour, L.L., Mitra, P.P., Kleinberg, R.L., Sotak, C.H., 1993. Time-dependent diffusion coefficient of fluids in porous media as a probe of surface-to-volume ratio. J. Magn. Reson. 101, 342-346.

Laxminarayana, C. Crosdale, P.J. 1999. Role of coal type and rank on methane sorption characteristics of Bowen Basin, Australia coals, Int. J. Coal Geol. 40 (4), 309–325.

Li, W., Zhu, Y.M., Wang, G., Jiang, B., 2016a. Characterization of coalification jumps during high rank coal chemical structure evolution. Fuel. 185, 298-304.

Li, X.S., Ju, Y.W., Hou, Q.L., Lin, H., 2012. Spectra response from macromolecular structure evolution of tectonically deformed coal of different deformation mechanisms. Science China Earth Sciences. 55, 1269-1279.

Li, X.J., Hayashi, J.I., Li, C, Z., 2006. FT-Raman spectroscopic study of the evolution of char structure during the pyrolysis of a Victorian brown coal. Fuel. 85, 1700-1707.

Li, Z.Q., Liu, Y., Xu, Y.P., Song, D.Y., 2016b. Gas diffusion mechanism in multi-scale pores of coal particles and new diffusion model of dynamic diffusion coefficient. Journal of China Coal Society. 41, 633-643.

Li, Z.Q., Wang, S.J., Liu, Y.W., Song, D.Y., Wang, Y.G, 2015. Coal gas diffusion mechanism based on dynamic diffusion coefficient new diffusion model. Journal of China University of Mining & Technology. 44, 836-842.

Liu, T., and Lin, B.Q., 2019. Time-dependent dynamic diffusion processes in coal: Model development and analysis. International Journal of Heat and Mass Transfer. 134, 1-9.

Liu, Z.J., Zhang, Z.Y., Choi, S.K., Lu, Y.Y., 2018a. Surface Properties and Pore Structure of Anthracite, Bituminous Coal and Lignite. Energies. 11, 1502.

Liu, Y., Zhu, Y.M., Liu, S.M., Chen, S.B., Li, W., Wang, Y., 2018b. Molecular structure controls on micropore evolution in coal vitrinite during coalification. Int. J. Coal Geol. 199, 19-30.

Meng, Y., Li, Z.P., 2018. Experimental comparisons of gas adsorption, sorption induced strain, diffusivity and permeability for low and high rank coals. Fuel. 234, 914-923.

Merkel, A., Gensterblum, Y., Krooss, B.M., Amann, A., 2015. Competitive sorption of CH_4, CO_2 and H_2O on natural coals of different rank. Int. J. Coal Geol. 150-151, 181-192.

Nie, B.S., Liu, X.F., Yang, Y.L., Meng, J.Q., Li, X.C., 2015. Pore structure characterization of different rank coals using gas adsorption and scanning electron microscopy. Fuel. 158, 908-917.

Pan, Z.J., Connell, L.D., Camilleri, M., Connelly, L., 2010. Effects of matrix moisture on gas diffusion and flow in coal. Fuel. 89, 3207-3217.

Pan, Z.J, Connell, L.D., 2012. Modelling permeability for coal reservoirs: a review of analytical models and testing data. Int J Coal Geol, 92, 1-44.

Sadezky, A., Muckenhuber, H., Grothe, H., Niessner, R., Poschl, U., 2005. Raman microspectroscopy of soot and related carbonaceous materials: Spectral analysis and structural information. Carbon. 43, 1731-1742.

Schwan, J., Ulrich, S., Batori, V., Ehrhardt, H., Silva, S.R.P., 1996. Raman spectroscopy on amorphous carbon films. J Appl Phys, 80(1): 440-447.

Smith, M.W., Dallmeyer, I., Johnson, T.J., Brauer, C.S., Mcewen, J.S., Espinal, J.F., 2016. Structural analysis of char by Raman spectroscopy: Improving band assignments through computational calculations from first principles. Carbon, 100: 678-692.

Tang, X., Li, Z., Ripepi, N., Louk, A. K., Wang, Z., Song, D., 2015. Temperature-dependent diffusion process of methane through dry crushed coal. Journal of Natural Gas Science and Engineering, 22, 609-617.

Tao, S., Chen, S.D., Tang, D, Z. Zhao, X., Xu, H., Li, S., 2018. Material composition, pore structure and adsorption capacity of low-rank coals around the first coalification jump: A case of eastern Junggar Basin, China. Fuel. 211, 804-815.

Valiullin, R., Skirda, V., 2001. Time dependent self-diffusion coefficient of molecules in porous media. J. Chem. Phys. 114, 452-458.

Wang, F., Cheng, Y.P., Lu, S.Q., Jin, K., Zhao, W., 2014. Influence of Coalification on the Pore Characteristics of Middle–High Rank Coal. Energy Fuels. 28, 5729-5736.

Wang, Z.F., Tang, X., Yue, G.W., Kang, B., Xie, C., Li, x., 2015. Physical simulation of temperature influence on methane sorption and kinetics in coal: Benefits of temperature under 273.15K. Fuel. 158, 207-216.

Yue, G.W., Wang, Z.F., Xie, C., Tang, X., Yuan, J.W., 2017. Time-Dependent Methane Diffusion Behavior in Coal: Measurement and Modeling. Transp. Porous Media. 116, 319-333.

Zhang, D.F., Cui, Y.J., Liu, B., Li, S.G., Song, W.L., Lin, W.G., 2011. Supercritical Pure Methane and CO_2 Adsorption on Various Rank Coals of China: Experiments and Modeling. Energy & Fuels. 25, 1891-1899.

Zhao, W., Cheng, Y.P., Jiang, H.N., Wang, H.F., Li, W., 2017. Modeling and experiments for transient diffusion coefficients in the desorption of methane through coal powders. Int. J. Heat Mass Transfer. 110, 845-854.

Zhao, W., Cheng, Y.P., Pan, Z.J., Wang, K., Liu, S.M., 2019. Gas diffusion in coal particles: A review of

mathematical models and their applications. Fuel. 252, 77-100.
Zhou, S.D., Liu, D.M., Cai, Y.D., Yao, Y.B., 2017. Effects of the coalification jump on the petrophysical properties of lignite, subbituminous and high-volatile bituminous coals. Fuel. 199, 219-228.

*Declaration of Interest Statement

Declaration of interests

The authors declare that they have no known competing financial interests or personal relationships that could have appeared to influence the work reported in this paper.

Highlights:

1) Behavior of methane diffusion in middle-high rank coals were characterized.

2) With the R_o increases, gas desorption capacity decreases first and then increases.

3) Evidence is presented to show that initial diffusion coefficient jumps at R_o=1.26%.

4) Raman parameter I_{D1}/I_G show a significant influence on behavior of diffusion in coal.

Influence of coalification on methane diffusion dynamics in middle-high rank coals

Jiang, Jingyu

2025

Jiang J, Zhang S, Longhurst P, et al., (2025) Influence of coalification on methane diffusion dynamics in middle-high rank coals. Energy Sources, Part A: Recovery, Utilization and Environmental Effects, Volume 47, Issue 1, 2025, pp. 4563-4577

https://doi.org/10.1080/15567036.2020.1871449